Axial Distribution of Reactivity Inside a Fluid-Bed Contactor

The axial distribution of reactivity inside a fluid-bed contactor is studied for the hydrogenation of ethylene. The reactivity is large near the surface of the dense phase. The significant effect of the dilute phase, or the free board region, is verified experimentally, and the contact efficiency in the transition zone and in the dilute phase is obtained. The contact efficiency was approximated by $\eta_c = 1 - 0.75(\epsilon_e/\epsilon_{ede})^{0.4}$. The temperature rise in the dilute phase is measured in the small reactor. The transition zone between the dense and dilute phases is almost isothermal, but it is found that temperature increases in the dilute phase.

SHINTARO FURUSAKI
TATSUJI KIKUCHI
and
TERUKATSU MIYAUCHI

Department of Chemical Engineering
University of Tokyo
Tokyo, Japan 113

SCOPE

Many models describing the reaction in fluid-bed contactors have been proposed that are based on the two-phase concept (Shen and Johnstone, 1955; Mathis and Watson, 1956; Lewis et al., 1959; Orcutt et al., 1962; Partridge and Rowe, 1966; Kobayashi et al., 1969; Kunii and Levenspiel, 1969; Kato and Wen, 1969; Mori and Muchi, 1972; Toei et al., 1972). Some of the models originate from basic studies on the behavior of bubbles inside the bed, and these are referred to as physical bubble models by Rowe (1972) who compared them with arbitrary two-phase models. A comparison of these models shows that the main differences between these models are related to whether or not some fraction of the catalyst is in direct contact with the bubble gas, the extent of axial mixing in each phase, and the axial change in bubble size.

Recently, Miyauchi (1974 *a*, *b*) proposed the concept of successive contact, taking account of catalyst particles suspended above the dense bed. This effect is important because of the good contact in the suspending zone (called the dilute phase). According to this theory, the reaction proceeds first in the dense phase in poor contact with the catalyst, then in the dilute phase in good contact. According to the theory, Miyauchi and Furusaki (1974) calculated conversions using the HRU or the contact efficiency. Experimental data previously obtained (Lewis et al., 1959; Van Swaay and Zuiderweg, 1972) were compared successfully with the calculation. The importance of the catalyst suspended in the dilute phase in controlling the selectivity was also discussed.

This paper presents experimental verification of the successive contact by the hydrogenation of ethylene on MS-Ni catalyst. This proof is essential in pursuing the analysis of fluid-bed contactors and is examined in detail. If the efficiency in the dilute phase is much higher than that in the dense phase as shown above, control of the reactivity in the dilute phase by the use of fines is considered useful in determining the optimal operation of fluid-bed contactors. This seems one of the reasons of utilizing fine particles in a fluid bed. This point is briefly discussed.

CONCLUSIONS AND SIGNIFICANCE

In studying the operation of a fluid-bed reactor by the concept of the successive contact, it is important to study the axial distribution of reactivity inside the bed. This is done by moving the axial position of the nozzle, through which one of the reactants, C_2H_4, is introduced into the fluid bed. By this method, the reactivity in the dilute phase is proved large, especially for the case of large reaction rates. The transition zone between the dense and dilute phases is found to be quite effective. The effective reactivity in the transition zone and in the dilute phase is attributed to the direct contact of solid and gas upon the burst of bubbles near the surface of the dense bed and to the direct contact between the gas and suspended solids in the upper region of the reactor, that is, the dilute phase. The contact efficiency in the dilute phase and transition zone is calculated from the experimental data. The efficiency increases from a point below the surface of the dense phase, as shown in Figure 6. It is a function of the bed density or the volume fraction of the emulsion and is approximated by $\eta_c = 1 - 0.75\ (\epsilon_e/\epsilon_{ede})^{0.4}$. This expression shows that η_c decreases rapidly with the increase of ϵ_e or ρ_b, the bed density in the dilute phase, probably due to the interference by solid particles with the transfer of the reactant gas.

A significant effectiveness in the transition zone and the dilute phase suggests the important role of fine particles in the operation of fluid-bed contactors. Calculations show that the use of relatively active fine particles leads to a more efficient use of catalyst and reactor. This was also shown by experiments. These results point to a desirable direction of developing fluid-bed reaction systems.

Fluidized beds are roughly classified into fluid-beds and teeter-beds (Squires, 1962; Ikeda, 1963). Teeter-beds contain rather large particles and are operated under relatively low gas velocities ($U_f/u_t < 1$). These are usually used in solid treatment operations such as gas-solid reactions, gasification of solid particles, drying, granulation, etc. Studies on teeter-beds have been carried out extensively by many investigators, and most of the results for the fluidized beds were obtained for the teeter beds. On the other hand, fluid-beds are operated under high gas velocities with small particles ($U_f/U_{mf} \geqq 100$, $U_f/u_t = 1 \sim 3$). Studies on fluid beds have been limited in num-

ber, and care must be taken in applying the results which were obtained from the experiments on the teeter-beds.

Catalytic reactions in fluidized bed reactors are usually conducted in the fluid-bed reactors (Squires, 1962; Ikeda, 1963). General features of a fluid-bed are given by these articles and also by Miyauchi and Furusaki (1974). One of the identifying features of a fluid-bed is the existence of fine particles ($d_p \leq 44$ μm). The amount of fines to give the characteristics of the fluid-bed is considered to be at least more than 10% by weight of the particles. If the amount is less than this value, the bed loses the specific flow features of fluid-bed even in case of microspherical particles. Thus, the role of fines is important for giving the desirable flow characteristic to the fluid-bed reactors.

The fluid-bed consists of the dense phase and the dilute phase; the latter is the phase of suspended particles above the dense phase and may also be referred to the freeboard region. The dense phase consists of the bubble phase and the emulsion phase and can be treated by the usual two-phase concepts. Intense circulation of the dense phase results from the buoyant force induced between the centrally ascending bubble rich region and the peripherally descending emulsion phase (Lewis et al., 1962; Miyauchi and Morooka, 1969*b*; Morooka et al., 1971). The behavior resembles that in gas bubble columns (Towell et al., 1965). Considering the effect of the dilute phase, Miyauchi (1974 *a, b*) suggests an equation to calculate the conversion of a fluid-bed reactor with the following assumptions.

1. There are constant ascending velocities for the bubble phase and circulating velocities for the emulsion phase. There is a transfer of gases between the ascending and descending emulsion and also between the bubble and emulsion.
2. The reactant gas rises through the ascending region by the form of bubbles.
3. In the dilute phase ($z \geqq L_f$) gases flow in the mode of piston flow and contact with catalyst particles.
4. The value of ϕ, which will be explained in later section, is more than 10. Then the effect of the circulating flow in the emulsion phase can be neglected:

$$C_{fo}/C_f^o = \exp(-N_{oR}) \tag{1}$$

$$N_{oR} = \frac{L_f}{U_f}\left\{\frac{1}{1/k_{ob}a_b + 1/\xi\epsilon_{ede}k_r} + (\mu\epsilon_b + e)k_r\right\} \tag{2}$$

is expressed by the volume fraction of emulsion in the paper. The importance of the effect of the variable e is discussed in Miyauchi and Furusaki (1974). This value is calculated by $\int_1^{z_t} \epsilon_e dZ$. In this case, ϵ_e for the dilute phase means the volume fraction of the solid phase whose apparent density is $\epsilon_{se}\rho_s$. Thus, ϵ_e is calculated by ρ_b/ρ_e or $\rho_b/\rho_s\epsilon_{se}$. Since the reaction rate constant k_r is usually expressed by

$$\left(\frac{\text{volume of the reactant consumed}}{\text{time}}\right)$$

(volume of the emulsion),

the expression of solid fraction in the dilute phase by ϵ_e is convenient in calculating the reactor performance.

EXPERIMENTAL OBSERVATION OF THE EFFECT OF THE DILUTE PHASE

Apparatus and Reaction

The experimental apparatus is shown in Figure 1. The reactor is made of stainless steel. The temperature is controlled by the boiling solution of ethylene glycol and water

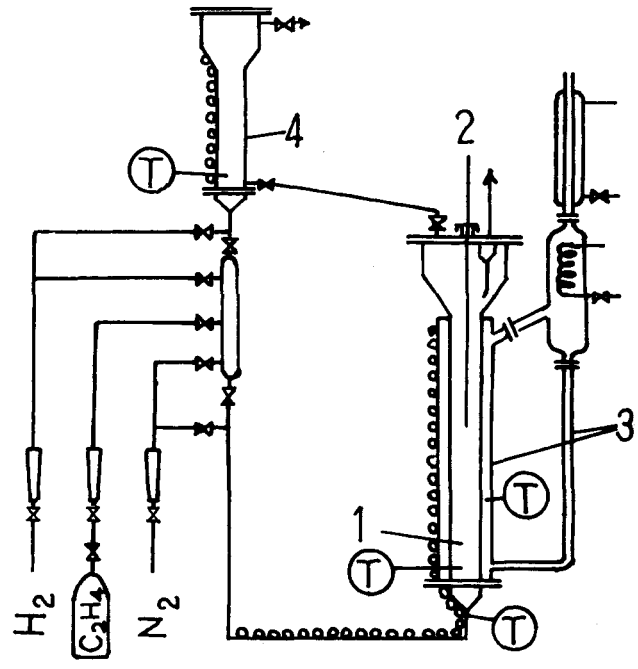

Fig. 1. Experimental apparatus; 1, reactor, 2, probe rod, 3, ethylene glycol solution, 4, catalyst reducer, T, thermocouple.

in the jacket. The jacket temperature is adjusted to about 140°C, which is the boiling point of 90 vol % solution of ethylene glycol. The diameter of the reaction zone is 5.3 cm and height is 130 cm. Above the reaction zone, there is the settling zone (20 cm diameter) and a cyclone to separate solid particles from the off gas. The distributor is a perforated plate of 2 mm holes with a stainless steel net of 325 mesh. The free area of the plate is about 4.9%. Below the distributor there is a bed of glass bead in order to regulate the flow of gas. A probe to measure temperature and static pressure inside the bed can be moved along the center by a rod of 5 mm diameter.

The reaction studied is the hydrogenation of ethylene with a nickel catalyst impregnated on an FCC (silica alumina) catalyst; that is

$$C_2H_4 + H_2 \xrightarrow{Ni} C_2H_6 \tag{3}$$

The heat of the reaction is −32.7 Kcal/mole at 25°C. The concentration of gas was 0.5 ~ 4% ethylene and the remainder hydrogen. The reaction rate was measured in a small fixed-bed reactor (1.8 mm diameter and 4 cm long) dipped in an isothermal vessel. In this low concentration of ethylene, the reaction was found to be pseudo first-order (Brammer et al., 1967). The apparent energy of activation is very low (0 ~ 4 Kcal/mole), and the reaction rate dependence on temperature can be ignored.

Conversions were measured by gas chromatography with a column of silica-gel and active charcoal.

Catalyst Preparation

Enough $Ni(COO)_2$ was used to make up 4% as nickel of the total catalyst. This was dissolved in concentrated NH_3 (aqueous solution), the volume of which is about 75% of the carrier. The solution was poured onto the carrier to soak it. This was dried and can be stored. Before use, the particles were charged into the reducer and decomposed at 250°C in a hydrogen stream for about 8 hr.

The carrier was silica alumina catalyst or FCC; the weight averaged diameter was 62 μm. The content of fine particles ($d_p \leq 44$ μm) was 22 wt %. The minimum

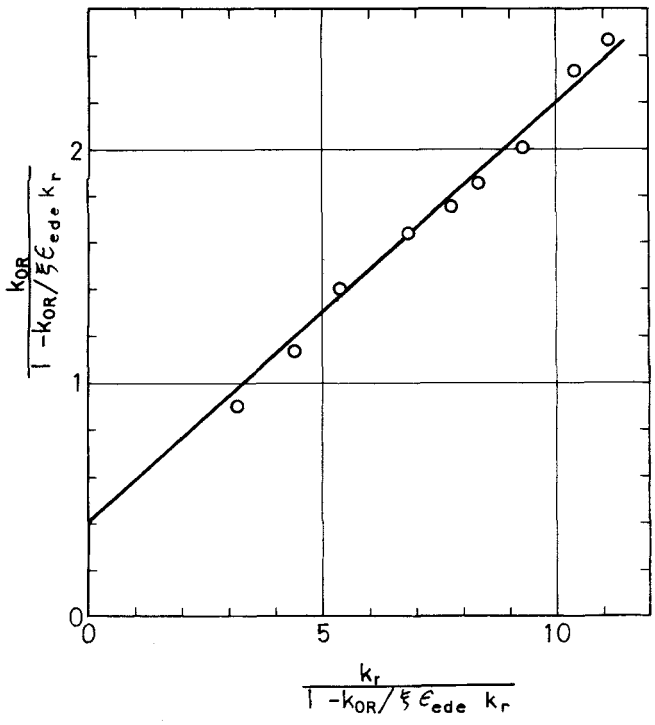

Fig. 2. Lewis-Gilliland-Glass plot for the reaction; U_f = 30.5 cm/s, catalyst 600 cm³.

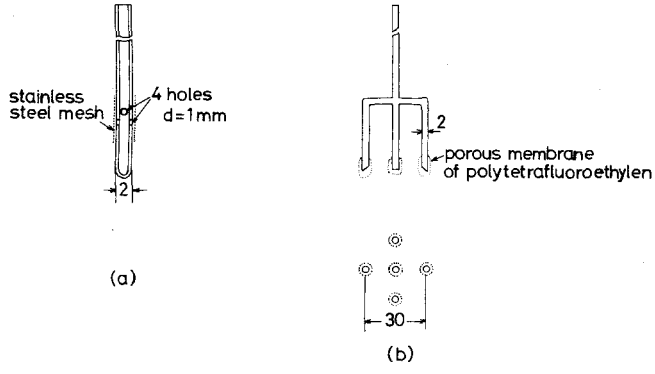

Fig. 3. Nozzles to inject ethylene; (a) 1 pipe, (b) 5 pipes.

fluidization velocity by air at room temperature was 0.2 cm/s.

Determination of $k_{ob}a_b$ by Means of the Lewis-Gilliland-Glass Plot

Lewis et al. (1959) presented an ingenious plot to separate the mass transfer term and the direct contact term using the conversions by catalysts of various activities. Applying their method to the successive contact model, we obtained the mass transfer term and the direct contact term.

Reaction proceeded in the reactor for U_f = 30.5 cm/s and a catalyst volume of 600 cm³. Catalyst activities were adjusted by adding inactive carrier particles. Conversions for different activities, but for the same operating conditions, were measured. N_{oR} was calculated by Equation (1), and the overall reaction rate k_{oR} was calculated by

$$k_{oR} = N_{oR}U_f/L_f \tag{4}$$

Equation (2) is arranged for convenience as follows:

$$k_{oR}k_r = \left(k_r - \frac{k_{oR}}{\xi\epsilon_{ede}}\right)k_{ob}a_b + k_r^2(\mu\epsilon_b + e) + \frac{k_rk_{ob}a_b(\mu\epsilon_b + e)}{\xi\epsilon_{ede}} \tag{5}$$

For $1 >> \frac{\mu\epsilon_b + e}{\epsilon_{ede}}$ or $k_r >> \frac{k_{ob}a_b}{\xi\epsilon_{ede}}$, the term

$$\frac{k_rk_{ob}a_b(\mu\epsilon_b + e)}{\xi\epsilon_{ede}}$$

can be neglected. Then

$$\frac{k_{oR}}{1-k_{oR}/\xi\epsilon_{ede}k_r} = \left(\frac{k_r}{1-k_{oR}/\xi\epsilon_{ede}k_r}\right)(\mu\epsilon_b + e) + k_{ob}a_b \tag{6}$$

Thus, a plot of $\frac{k_{oR}}{1-k_{oR}/\xi\epsilon_{ede}k_r}$ vs. $\frac{k_r}{1-k_{or}/\xi\epsilon_{ede}k_r}$ gives a straight line with the intercept $k_{ob}a_b$ and slope $\mu\epsilon_b + e$. This is given by Figure 2 for the present data measured as above. From the figure, $k_{ob}a_b$ is found around 0.4 s^{-1}, and $\mu\epsilon_b + e$ is about 0.16 for U_f = 30 cm/s. When we consider that μ is very small, e is about 0.16.

Miyauchi (1974*a*) proposed a method to determine e by means of the static pressure measurement. In this method, e is defined as the amount of catalyst above the point f, where ϵ_b = 0.5 divided by the amount of catalyst below the point. The value thus obtained was 0.17, very close to that obtained by the Lewis-Gilliland-Glass plot.

The Lewis-Gilliland-Glass plot modified from the original one (Lewis et al., 1959) can thus be used for catalysts of high activities. For small values of e or large values of k_r, this method can be used effectively.

Axial Distribution of Reactivity along the Center of the Bed

The axial distribution of reactivity can be measured by several methods. In this paper, a method is presented so that one of the reactants (C_2H_4) is charged from an inlet nozzle traveling longitudinally along the central axis. From a sample from the outlet, the dependence of conversions on the height of the nozzle was measured. This gives the information on the distribution of local apparent overall reactivity.

Before applying this method, the experiments feeding the whole reactant gas through the distributor were carried out. The conversions with the different bed height agreed with the calculated values by the successive contact model. Also, the axial concentration profiles through the bed were investigated. In carrying out this experiment for the fluid bed, where the gas flow rate is considerably high, the samples of the bubble gas were difficult to obtain. Therefore, the concentration of the bubble phase was calculated from the overall sample of the dense phase by using the bubble frequency data measured by the hot wire probe method (Morooka et al., 1971). The concentration profile thus obtained was successfully compared with the calculation (Furusaki et al., 1975). However, the axial distribution of the reactivity was most clearly observed by the method here presented.

It is interesting to note the features of flow when one applies this method to a fluid bed. If the nozzle is located in the dilute phase, the gas from the nozzle will be mixed with the gas ascending from the bottom. This case is straightforward with the assumption of piston flow. If the nozzle is located in the dense phase, there are two cases. One is the case when the gas from the nozzle is mixed with the bubble. In this case, the only problem is whether or not the gas mixes immediately with the gas in the bubble. In this paper this is assumed, since a strong disturbance exists inside the dense phase. This was examined by changing the shape of the nozzle as shown later. The other case is when the gas from the nozzle is blown into the emulsion and rises as small bubbles. The size of bubbles is calculated by the Davidson and Schuler equation (1960)

and the method of Miyauchi and Yokura (1972) and is found to be about 0.5 ~ 1 cm. These bubbles probably coalesce immediately with larger bubbles ascending from the bottom, because the rise velocity of these small bubbles formed from the nozzle is very small. Hence, if mixing inside the bubble is violent enough, the gas blown from the nozzle can be considered to be fed into the bubble phase.

The shapes of the nozzle are shown in Figure 3. The nozzle (b) is designed to inject the gas as uniformly as possible into the ascending zone. There was no difference in the results for the two types of nozzles when they were held in the dense phase. This is probably due to the violent turbulence in the bed. The conversion was little higher for the nozzle (b) than (a) when they were held in the dilute phase because some portion of the gas injected through the nozzle (b) enters the descending periphery. Most of the experiments were made with nozzle (a).

Gas mixing is ignored in pursuing this method according to Miyauchi and Morooka (1969*b*). They investigated the effect of the circulating flow inside the dense bed and presented a criterion for neglecting the circulation of the gas phase. That is, the value of

$$\phi = \frac{U_f}{m_c U_e}\left(1 + 4m_c \frac{k_{ex}\, a_{ex}}{k_{ob}\, a_b} + \frac{\epsilon_{ede}\, k_r}{k_{ob}\, a_b}\right)$$

must be greater than 10. The value of ϕ in this experiment is calculated to be 25 ~ 63 for U_f = 10 ~ 40 cm/s.

Examples of data obtained are given in Figures 4 and 5. Figure 4 shows data for 1 000 cm³ of the catalyst. Point *f*, where ϵ_e = 0.5 according to Miyauchi (1974*a*), is 61 cm above the distributor for U_f = 9.9 cm/s, and 66 cm for U_f = 30.5 cm/s. [Point *f* is in the transition zone between the dense and dilute phase as shown in Figure 1 of Miyauchi and Furusaki (1974). Therefore, this ϵ_e has the same meaning as stated in the earlier part of this paper for case of the dilute phase.] From these data in the figure, it is quite obvious that the relative overall reactivity is large near point *f*. By assuming the plug flow of the gas as the successive contact model, the material balance equation is as follows:

$$-U_f \frac{dC}{dz} - r(C) = 0 \tag{7}$$

If the reaction rate $r(C)$ is the product of the function of the height and that of concentration, then

$$-U_f \frac{dC}{dz} - k_{oR}(z)\, f(C) = 0 \tag{8}$$

From this

$$\int_z^{L_t} \frac{k_{oR}(z)}{U_f}\, dz = -\int_{C_{f^o}}^{C_{fo}} \frac{dC}{f(C)} \tag{9}$$

Differentiating by z, we get

$$\frac{k_{oR}(z)}{U_f} = \frac{d}{dz}\int_{C_{f^o}}^{C_{fo}} \frac{dC}{f(C)} \tag{10}$$

Equation (10) is the general equation to obtain the local overall reactivity k_{oR} from this experiment. If the kinetics are first order, that is, $f(C) = C$, then

$$\frac{k_{oR}(z)}{U_f} = \frac{d}{dz}\left\{\ln\left(\frac{C_{fo}}{C_f{}^o}\right)\right\} \tag{11}$$

Thus, the differential of the ordinate of Figure 4 represents the local reactivity. For the dense phase, from Equations (1) and (2), we get

$$\frac{d}{dz}\left\{\ln\left(\frac{C_{fo}}{C_f{}^o}\right)\right\} = \frac{k_{or} + \mu\epsilon_b\, k_r}{U_f} \tag{12}$$

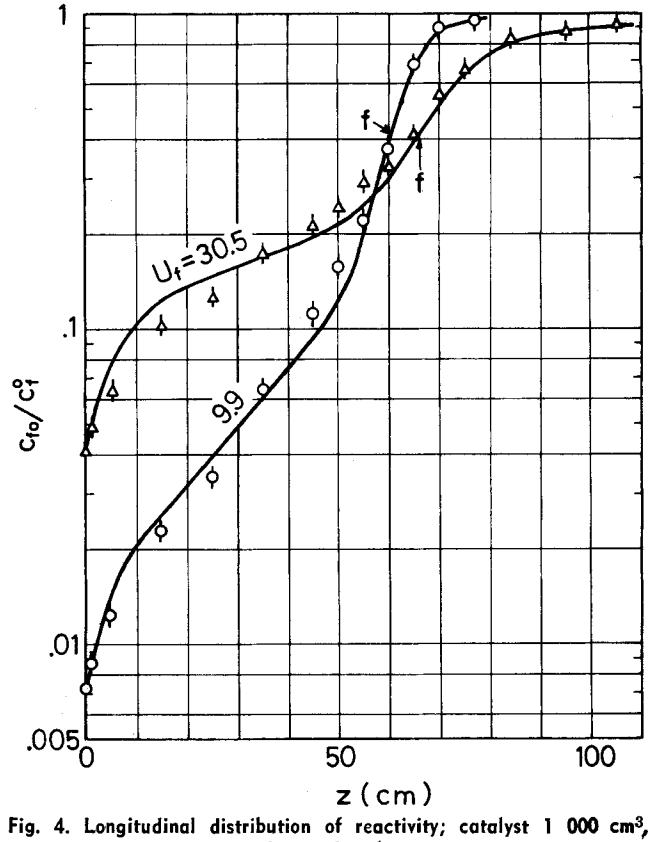

Fig. 4. Longitudinal distribution of reactivity; catalyst 1 000 cm³, k_r = 10 s⁻¹.

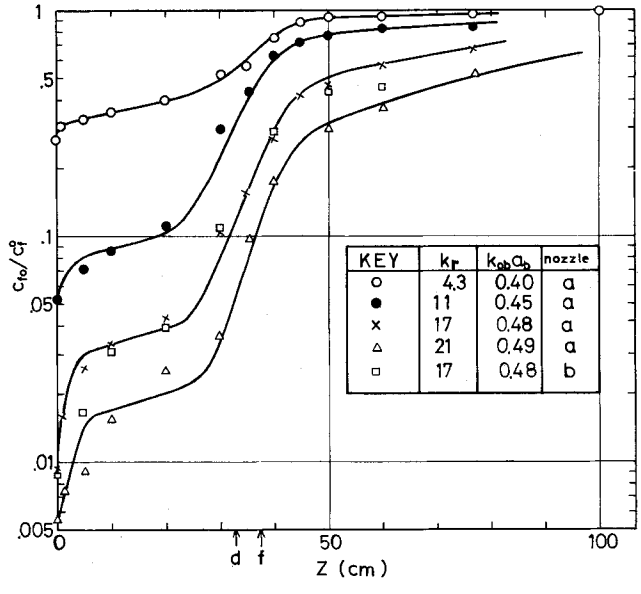

Fig. 5. Effect of the reaction rate to the longitudinal distribution of reactivity, catalyst 600 cm³, U_f = 30.5 cm/s.

where $k_{or} = \dfrac{1}{1/k_{ob}\, a_b + 1/\xi\epsilon_{ede}\, k_r}$. For the dilute phase, we get

$$\frac{d}{dz}\left\{\ln\left(\frac{C_{fo}}{C_f{}^o}\right)\right\} = \frac{\eta_c\, \epsilon_e\, k_r}{U_f} \tag{13}$$

Here, η_c is the local contact efficiency defined by Equation (13). It can be used for the dense phase and equals $\eta_{cde} = \dfrac{\mu\epsilon_b}{\epsilon_{ede}} + \dfrac{1}{\epsilon_{ede}k_r/k_{ob}a_b + 1/\xi}$. By using Equation (12), the slope of the curve for the dense phase in Figure 4 can be found from the value of $k_{ob}a_b$. The solid lines are thus obtained, if we assume that μ = 0, ξ = 1, and $k_{ob}a_b$ = 0.4 s⁻¹ for U_f = 30.5 cm/s. The effect of the reaction rate on

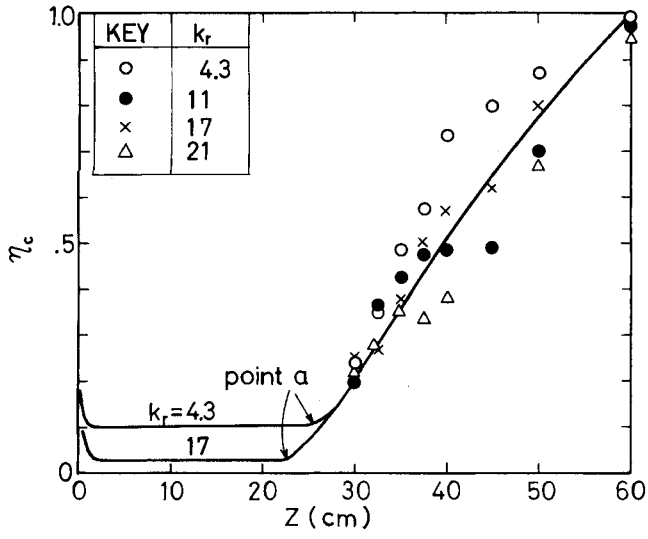

Fig. 6. Dependence of η_c on the height from the distributor; catalyst 600 cm^3, U_f = 30.5 cm/s.

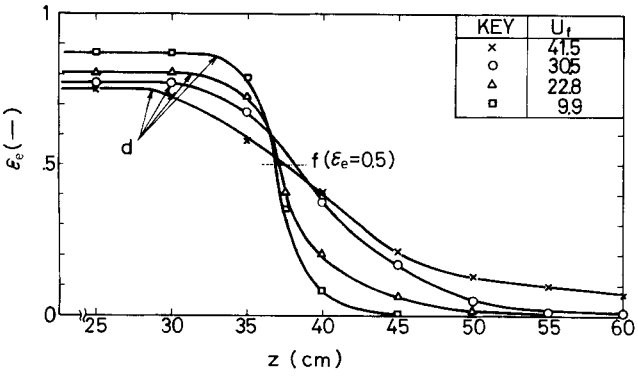

Fig. 7. Bed density by static pressure measurement; catalyst 600 cm^3.

the mass transfer, the Hatta number, is taken into consideration in calculating $k_{ob}a_b$ by assuming that the mass transfer resistance in the emulsion side is 1.73 times larger than that in the bubble side. [This 1.73 comes from $k_b = \frac{2}{\sqrt{\pi}}\sqrt{D_G/\tau_b}$, $k_e = \frac{2}{\sqrt{\pi}}\sqrt{mD_{\text{eff}}/\tau_b}$ (Miyauchi and Morooka, 1969*a*). Here, $m \approx 1$, $D_{\text{eff}} = \epsilon_{fe} D_G/\chi \doteqdot \frac{D_G}{3}$. The calculating procedure is stated in Miyauchi and Furusaki (1974) and Miyauchi (1974b).] η_c for the dilute phase is obtained from the tangent of the curve. This will be discussed later. The best fit of the data was obtained by assuming $\mu = 0.05 \sim 0.1$. The value of μ is probably larger than zero owing to coalescence of bubbles but cannot be determined by direct measurements. Hence, $\mu = 0$ is assumed for the first approximation.

Near the distributor, the contact seems to be more effective than in other portions of the dense phase. One of the reasons for this is probably direct contact of solid and gas in case of coalescence of bubbles (Shichi et al., 1968; Toei et al., 1969; Clift and Grace, 1972). There might be an influence of poor distribution of the gas from the nozzle, that is, ethylene from the nozzle may not mix with hydrogen immediately in the bed, so this effect may be exaggerated. Apparently, the contact efficiency at 0 ~ 8 cm above the distributor is about 20 ~ 30%.

The effects of the reaction rate are shown in Figure 5. The data can be explained by the theory, and the calculated values are shown by the solid lines in the figures. η_c calculated from the data of Figure 5 is shown in Figure 6. Comparing this η_c with the bed density in Figure 7, one finds that η_c starts growing at point *a*, which is a little below point *d*. (Point *d* is the point where the bed density starts decreasing.) This means that the disturbance at the surface of the dense bed affects the behavior of the bed below the surface.

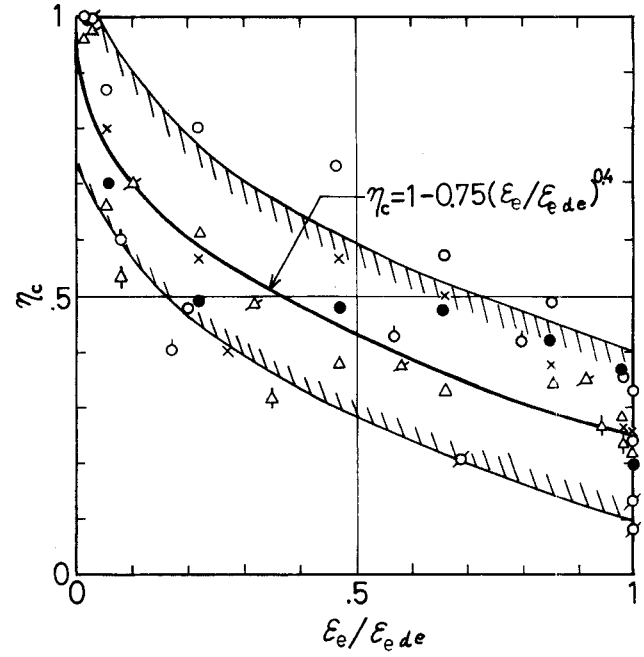

Fig. 8. Correlation of the contact efficiency with $\epsilon_e/\epsilon_{ede}$.

The mechanism of contact in the dilute phase (including the transition zone) is considered in the following way. Agglomerates of catalyst particles are blown up when bubbles break. Catalysts spill down from the agglomerates as they ascend in the reactor. The contact efficiency η_c is a function of the fraction of gas flow through the agglomerate, mass transfer rate between the agglomerate and the lean phase, and the volume fraction of solid particles inside the agglomerate and the lean phase.

In other words, the contact efficiency is expected to be a function of mutual interference of the particle movement. When the viscous force prevails, the forces which work on small particles are affected strongly by the void fraction in the space (Steinour, 1944; Lewis et al., 1949). The particle Reynolds number is well in the Stokes flow region. Also, the hindered settling of the particle swarm is primarily governed by the volume fraction of particles ϵ_s (Zuber, 1964). Upon these considerations, the contact efficiency is considered to be a function of the volume fraction of solid particles or ϵ_e. When we normalize by ϵ_{ede}, $\epsilon_e/\epsilon_{ede}$ or ρ_b/ρ_{bde} is chosen as a variable to affect η_c because this is a primary data which can be obtained by the measurement of the solid density in the bed. Here, ϵ_{ede} is the volume fraction of the emulsion in the dense phase and considered to be a constant for a given condition. The value of η_c is shown in Figure 8 against $\epsilon_e/\epsilon_{ede}$. Most of the efficiencies calculated from Figures 4 and 5 are inside the shadow in Figure 8. The most probable value is given by the solid line in the figure. The mathematical relationship is

$$\eta_c = 1 - 0.75\ (\epsilon_e/\epsilon_{ede})^{0.4} \qquad (14)$$

Equation (14) shows that the strong interaction of particles affects the contact efficiency. The interaction seems to increase rapidly with increasing particle population as in the case of sedimentation (Zuber, 1964).

Table 1. Effect of Fine Particles on Conversion

No.	Dilution	Constitution	Percentage of fines	k_r for active particle	Conv.
1	20% active 80% inactive	Same activity for any size.	22	ca8	0.417
2	20% active 80% inactive	Fine is active. Inactive particles are FCC catalysts without fines.	20	ca8	0.691

In calculating η_c, the above equation can be used. Attention is necessary because η_c is larger than η_{cde} at the point $\epsilon_e/\epsilon_{ede} = 1$ (point d), as stated before. The convenient way to obtain η_c is as follows:

1. Measure the density in the bed by an appropriate method such as static pressure measurement or by the absorption of γ-rays or X-rays.
2. Calculate η_c from Equation (14).
3. Calculate η_{cde}.
4. Plot η_c and η_{cde} vs. z.
5. Extrapolate η_c for $z < L_d$. The point of intersection with the line of η_{cde} is point a. Between L_a and L_d, appropriate contact efficiency should be η_c instead of η_{cde}.

Recently, Chavarie and Grace (1975) have reported the abrupt increase of conversion near the surface of the fluidized bed of large particles, especially for the cases of large reaction rates. The similar good contact at the surface may occur in the teeter bed.

The method used here and Equation (11) may be applied to other apparatus with the end effects, such as liquid extraction columns, bubble columns, packed columns, trays, etc. In these cases, Equation (15) is the general relationship:

$$H_{oL} \cdot N_{oL} = Z \tag{15}$$

Hence

$$\frac{\partial N_{oL}}{\partial Z} = \frac{1}{H_{oL}} = \frac{K_{oL}a}{U_f} \tag{16}$$

Thus, the reactant (or absorbant) is fed from various longitudinal positions, and N_{oL} is calculated from the concentration at the outlet. Then, differentiation of N_{oL} with respect to the effective bed height will give the local value of H_{oL} or K_{oL}. This method is sometimes better than the measurement of the concentration profile when sampling from the definite phase is difficult.

TEMPERATURE PROFILES IN THE DILUTE PHASE

Since the contact efficiency in the dilute phase is better and the effective thermal conductivity is much lower than in the dense phase, a temperature rise in the dilute phase is expected. Miyauchi and Furusaki (1974) calculated the effect of temperature rise on the selectivity of several reaction models under the adiabatic condition. Experiments were carried out in order to examine the temperature rise. Some of the results are shown in Figure 9. Since the diameter of the reactor is very small and the reactor wall is maintained at a constant temperature, the temperature rise is rather small. But it is found that there is a temperature rise in the dilute phase. The reactor is cooled by the jacket of ethylene glycol solution, so the temperature in the reactor is generally decreasing as indicated in Figure 9. However, in an adiabatic reactor such as that used in industry, the temperature will continue to increase. Hence, the temperature in the dilute phase is expected to increase more than shown in this experiment. Also, it should be noted that just above the distributor the extent of reaction is large, and that the temperature is higher than the other portion of the dense phase.

The enthalpy balances for both the ascending and descending zones are given for the steady state in nondimensional form:

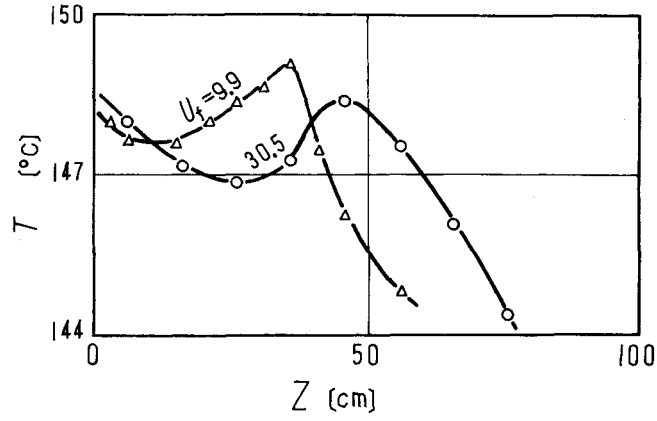

Fig. 9. Temperature rise in the dilute phase; catalyst is made by 100 cm³ of active ($k_r \doteq 8$) fines and 500 cm³ of inactive carrier particle without fines.

$$-(1+\lambda m)\frac{d\theta^{(u)}}{dZ} + \frac{1}{2}\eta_c\epsilon_e\Omega N_{Ar}e^{-\frac{\Gamma}{\theta^{(u)}}}C - N_H(\theta^{(u)} - \theta^{(d)}) = 0 \tag{17}$$

$$\lambda m\frac{d\theta^{(d)}}{dZ} + \frac{1}{2}\eta_c\epsilon_e\Omega N_{Ar}e^{-\frac{\Gamma}{\theta^{(d)}}}C + N_H(\theta^{(u)} - \theta^{(d)}) - N_w(\theta^{(d)} - \theta_w) = 0 \tag{18}$$

Here, the radial concentration distribution and the flow of the descending gas are neglected. If one assumes the adiabatic operation, then $N_w = 0$. Special cases arise when $N_H >> 1$ or $N_H \approx 0$. For $N_H >> 1$, $\theta^{(u)}$ is equal to $\theta^{(d)}$. Thus

$$-\frac{d\theta}{dZ} + \eta_c\epsilon_e\Omega N_{Ar}e^{-\frac{\Gamma}{\theta}}C = 0 \tag{19}$$

This is the same case as discussed by Miyauchi and Furusaki (1974). For $N_H \approx 0$, the ascending temperature is given by

$$-(1+\lambda m)\frac{d\theta^{(u)}}{dZ} + \frac{1}{2}\eta_c\epsilon_e\Omega N_{Ar}e^{-\frac{\Gamma}{\theta^{(u)}}}C = 0 \tag{20}$$

Thus, the ascending temperature profile is obtained in the same way as Equation (19) by substituting $\Omega/2(1+\lambda m)$ for Ω. The value of m is about 10^3; λ is 0.001 ~ 0.15 depending upon the value of ρ_b/ρ_{bde} or $\epsilon_e/\epsilon_{ede}$. Further study is under way and shall be reported subsequently.

THE EFFECT OF THE DISTRIBUTION OF THE REACTIVITY

The axial distribution of the reactivity has thus been verified experimentally. If one uses more active fine particles, one will obtain more effective dilute phase and higher conversions. Experimental measurements were performed to test this hypothesis, and the results are shown in Table 1. Comparing reaction 1 and 2, one can see that the use of a fine-active catalyst is more effective.

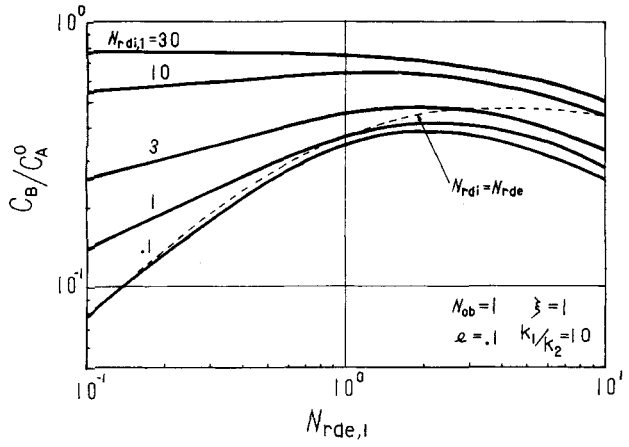

Fig. 10. Effect of active fines, isothermal irreversible first-order cumulative reaction, $A \xrightarrow{1} B \xrightarrow{2} C$.

The effect of fines on selectivity is shown in Figure 10. This is the result calculated by the successive contact model (Miyauchi, 1974*a*, *b*). The isothermal consecutive reaction ($A \xrightarrow{1} B \xrightarrow{2} C$) is studied. The yield of the desired product B is shown as a function of the number of reaction units in the dense and dilute phases. If the activities in the dilute phase are larger than those in the dense phase, the results are shown above the broken line. From the figure, it is found that the yield of B is larger when the reaction rate in the dilute phase is larger than that in the dense phase. For example, if N_r in the dense phase for the reaction 1, that is, $N_{rde,1}$, equals unity and the reaction rate in the dilute phase is ten times larger ($N_{rdi} = 10$), the yield improves from 36 to 64%. This is due to the fact that the mass transfer resistance increases the concentration of B in the emulsion and increases the amount to be reacted into C. Thus, the mass transfer resistance decreases the selectivity of the consecutive reaction. This result shows that the use of active fines improves the contact efficiency and gives higher selectivity. This also suggests the possibility of controlling the reaction zone in a fluid bed.

ACKNOWLEDGMENT

Experiments were carried out at Nishiki Factory of Kureha Chemical Industries, Ltd. The authors express their gratitude to Messrs. T. Arai, H. Washimi, and H. Kaji for the company's support in constructing the apparatus and in accomplishing the experiments.

NOTATION

A_r = frequency factor for the Arrhenius equation, s^{-1}
a = mass transfer area, cm^2/cm^3
a_b = mass transfer area between bubble and emulsion, cm^2/cm^3
a_{ex} = area of contact between the ascending and descending zone, cm^2/cm^3
a_w = area of heat transfer between wall and the descending zone, cm^2/cm^3
C = concentration, $gmole/cm^3$
C_f^o = reactant concentration in the inlet gas, $gmole/cm^3$
C_{fo} = reactant concentration in the outlet gas, $gmole/cm^3$
c_p = heat capacity, cal/g °C
D_G = molecular diffusivity of gas, cm^2/s
D_{eff} = effective diffusivity in the emulsion, $\epsilon_{fe} D_G/\chi$, cm^2/s
d_p = diameter of the particles, cm
E = activation energy, kcal/gmole
e = amount of catalyst particles in the dilute phase, dimensionless
$-\Delta H$ = heat of reaction, kcal/gmole
H_{oL} = overall height of a transfer unit, cm
h_{ex} = heat transfer coefficient between the ascending and descending zone, cal/cm^2 °C s
h_w = heat transfer coefficient between the wall and the descending zone, cal/cm^2 °C s
K_{oL} = overall mass transfer coefficient, cm/s
k_{ex} = mass transfer coefficient between the ascending and descending emulsion, cm/s
k_{ob} = overall mass transfer coefficient between the bubble and emulsion phase, cm/s
k_{oR} = overall reaction rate, s^{-1}
$k_{or} = \dfrac{1}{1/k_{ob}a_b + 1/\xi\epsilon_{ede}k_r}$, s^{-1}
k_r = reaction rate constant, s^{-1}
L_a = height of point a from the distributor, cm
L_d = height of point d from the distributor, cm
L_f = height of point f from the distributor, cm
L_t = total bed height, cm
$m = \dfrac{c_{ps}\rho_s}{c_{pf}\rho_f}$, dimensionless
m_c = adsorption equilibrium constant for the emulsion, dimensionless
$N_{Ar} = \dfrac{A_r L_f}{U_f}$, dimensionless
$N_H = \dfrac{h_{ex} a_{ex} L_f}{U_f c_{pf} \rho_f}$, dimensionless
N_{oR} = overall number of a reaction unit, dimensionless
$N_w = \dfrac{h_w a_w L_f}{U_f c_{pf} \rho_f}$, dimensionless
$r(C)$ = reaction rate, $gmole/s\ cm^3$
T = temperature, °C
T_d = temperature of the dense phase, °C
U_e = superficial circulation velocity of the emulsion phase, cm/s
U_f = flow rate of the gas, cm/s
U_{mf} = minimum fluidization velocity, cm/s
U_s = circulation rate of the solid, cm/s
u_t = terminal velocity of the particle, cm/s
Z = z/L_f, dimensionless
z = height from the distributor, cm

Greek Letters

Γ = E/RT_d, dimensionless
ϵ_b = volume fraction of the bubble phase, dimensionless
ϵ_e = volume fraction of the solid phase expressed as the emulsion, dimensionless
ϵ_{fe} = void fraction in the emulsion phase, dimensionless
η_c = contact efficiency in the dilute phase, dimensionless
η_{cde} = contact efficiency in the dense phase, dimensionless
θ = T/T_d, dimensionless
θ_w = T_w/T_d, dimensionless
λ = U_s/U_f, dimensionless
μ = fractional amount of catalyst particles in the bubble phase, dimensionless
ξ = effective fraction of catalyst in the dense phase, dimensionless
$\Omega = \dfrac{(-\Delta H)\, C_f^o}{c_{pf}\rho_f T_d}$, dimensionless
ρ_b = bed density, g/cm^3
ρ_{bde} = density of the dense phase, g/cm^3
τ_b = local surface renewal time between bubble and

emulsion, s

χ = tortuosity factor in the emulsion, dimensionless

Subscripts

b = bubble phase
de = dense phase
di = dilute phase
e = emulsion phase
f = gas
s = solid

Superscripts

d = descending zone
u = ascending zone

LITERATURE CITED

Brammer, K. R., K. Schugerl, and G. Sehiemann, "Umsatzprofile in Flieszbett-Reaktoren," *Chem. Eng. Sci.*, **22**, 573 (1967).

Chavarie, C., and J. R. Grace, "Performance Analysis of a Fluidized Bed Reactor. II Observed Reactor Behavior Compared with Simple Two-Phase Models," *Ind. Eng. Chem. Fundamentals*, **14**, 79 (1975).

———, "Performance Analysis of a Fluidized Bed Reactor. III Modification and Extension of Conventional Two-Phase Models," *ibid.*, 86 (1975).

Clift, R., and J. R. Grace, "Coalescence of Bubble Chains in Fluidized Beds," *Trans. Inst. Chem. Engrs.*, **50**, 364 (1972).

Davidson, J. F., and B. O. G. Schuler, "Bubble Formation at Orifice in an Inviscid Liquid," *ibid.*, **38**, 335 (1960).

Furusaki, S., T. Kikuchi, and T. Miyauchi, "Behavior of a Fluid Bed in the Hydrogenation of Ethylene," paper presented at Fukuoka Meeting, Soc. Chem. Engrs. Japan (Oct., 1974).

Ikeda, Y., "Problems in the Industrial Application of the Fluidized Catalytic Reaction," *Kagaku Kogaku*, **27**, 667 (1963).

Kato, K., and C. Y. Wen, "Bubble Assemblage Model for Fluidized Bed Catalytic Reactors," *Chem. Eng. Sci.*, **24**, 1351 (1969).

Kobayashi, H., F. Arai, T. Chiba, and Y. Tanaka, "Estimation of Catalytic Conversion in Gas-fluidized Beds by Means of Two-Phase Model," *Kagaku Kogaku*, **33**, 274 (1969).

Kunii, D., and O. Levenspiel, *Fluidization Engineering*, Wiley, New York (1969).

Lewis, W. K., E. R. Gilliland, and W. C. Bauer, "Characteristics of Fluidized Particles," *Ind. Eng. Chem.*, **41**, 1104 (1949).

———, and H. Girouard, "Heat Transfer and Solid Mixing in Beds of Fluidized Solids," *Chem. Eng. Progr. Symposium Ser. No. 38*, **58**, 67 (1962).

Lewis, W. K., E. R. Gilliland, and W. Glass, "Solid-Catalyzed Reaction in a Fluidized Bed," *AIChE J.*, **5**, 419 (1959).

Mathis, J. F., and C. C. Watson, "Effect of Fluidization on Catalytic Cumene Dealkylation," *ibid.*, **2**, 518 (1956).

Miyauchi, T., "Concept of Successive Contact Mechanism for Catalytic Reaction in Fluid Beds," *J. Chem. Eng. Japan*, **7**, 201 (1974*a*).

———, "Behavior of Successive Contact Mechanism for Catalytic Reaction in Fluid Beds," *ibid.*, 207 (1974*b*).

———, and S. Furusaki, "Relative Contribution of Variables Affecting the Reaction in Fluid Bed Contactors," *AIChE J.*, **20**, 1087 (1974).

Miyauchi, T., and S. Morooka, "Mass Transfer Rate between Bubble and Emulsion Phase in Fluid Bed," *Kagaku Kogaku*, **33**, 880 (1969*a*).

———, "Circulating Flow and its Effect on Chemical Reaction in Fluid Bed Contactors," *ibid.*, 369 (1969*b*); also in *Intern. Chem. Eng.*, **9**, 713 (1969*b*).

Miyauchi, T., and M. Yokura, "The Mechanism of Nucleate Boiling Heat Transfer," *Heat Transfer Japanese Research*, **1**, No. 2, 109 (1972).

Mori, S., and I. Muchi, "Theoretical Analysis of Catalytic Reaction in Fluidized Bed," *J. Chem. Eng. Japan*, **5**, 251 (1972).

Morooka, S., K. Tajima, and T. Miyauchi, "Behavior of Gas Bubbles in Fluid Beds," *Kagaku Kogaku*, **35**, 680 (1971); also in *Intern. Chem. Eng.*, **12**, 168 (1972).

Orcutt, J. C., J. E. Davidson, and R. L. Pigford, "Reaction Time Distributions in Fluidized Catalytic Reactors," *Chem. Eng. Progr. Symposium Ser. No. 38*, **58**, 1 (1962).

Partridge, B. A., and P. N. Rowe, "Chemical Reaction in a Bubbling Gas-Fluidized Bed," *Trans. Inst. Chem. Engrs.*, **44**, T335 (1966).

Rowe, P. N., "Fluidized Bed Reactors," Proc. of the Fifth European/Second International Symp. on Chem. Reaction Eng., Amsterdam. A9 (1972).

Shen, C. Y., and H. F. Johnstone, "Gas Solid Contact in Fluidized Beds," *AIChE J.*, **1**, 349 (1955).

Shichi, R., S. Mori, and I. Muchi, "Interaction between Two Bubbles in Gaseous Fluidization," *Kagaku Kogaku*, **32**, 343 (1968).

Squires, A. M., "Species of Fluidization," *Chem. Eng. Progr. Symposium Ser. No. 38*, **58**, 57 (1962).

Steinour, H. H., "Rate of Sedimentation," *Ind. Eng. Chem.*, **36**, 618 840 (1944).

Toei, R., R. Matsuno, K. Nishitani, H. Hayashi, and T. Imamoto, "Gas Interchange between Bubble Phase and Continuous Phase in Gas-Solid Fluidized Bed at Coalescence," *Kagaku Kogaku*, **33**, 668 (1969).

Toei, R., R. Matsuno, H. Hotta, M. Oichi, and Y. Fujine, "The Capacitance Effect on the Transfer of Gas or Heat Between a Bubble and the Continuous Phase in a Gas-solid Fluidized Bed," *J. Chem. Eng. Japan*, **5**, 273 (1972).

Towell, G. D., C. P. Strand, and G. H. Ackermann, "Mixing and Mass Transfer in Large Diameter Bubble Columns," paper presented at Am. Inst. Chem. Engrs. and Inst. Chem. Engrs., Joint Meeting, London, England (1965).

van Swaay, W. P. M., and F. J. Zuiderweg, "Investigation of Ozone Decomposition in Fluidized Beds on the Basis of a Two-Phase Model," paper presented at Symp. on Chem. Reaction Eng., Amsterdam (1972).

Zuber, N., "On the Dispersed Two-Phase Flow in the Laminar Flow Regime," *Chem. Eng. Sci.*, **19**, 897 (1964).

Manuscript received September 30, 1975; revision received and accepted November 28, 1975.

Digital Monitoring and Estimation of Polymerization Reactors

A free-radical polymerization with kinetic equations taking into account monomer, polymer, and solvent transfer and initiation, termination, propagation, and inhibition reactions was studied both experimentally and by simulation to determine the performance of various Kalman filters, with feasible measurements used.

J. H. JO

and

S. G. BANKOFF

Chemical Engineering Department
Northwestern University
Evanston, Illinois